Role of loop entropy in the force induced melting of DNA hairpin

Garima Mishra, Debaprasad Giri, M. S. Li, et al.

View Online   Export Citation

ARTICLES YOU MAY BE INTERESTED IN

Force induced melting of the constrained DNA
The Journal of Chemical Physics **132**, 235105 (2010); https://doi.org/10.1063/1.3427587

Force-induced rupture of double-stranded DNA in the absence and presence of covalently bonded anti-tumor drugs: Insights from molecular dynamics simulations
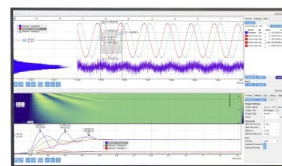The Journal of Chemical Physics **148**, 215105 (2018); https://doi.org/10.1063/1.5024975

Dynamics of a polymer under multi-gradient fields
The Journal of Chemical Physics **150**, 024906 (2019); https://doi.org/10.1063/1.5052219

Role of loop entropy in the force induced melting of DNA hairpin

Garima Mishra,[1] Debaprasad Giri,[2,a)] M. S. Li,[3] and Sanjay Kumar[1]

[1]*Department of Physics, Banaras Hindu University, Varanasi 221 005, India*
[2]*Department of Applied Physics, IT, Banaras Hindu University, Varanasi 221 005, India*
[3]*Institute of Physics, Polish Academy of Sciences, Al. Lotnikow 32/46, 02-668 Warsaw, Poland*

Dynamics of a single stranded DNA, which can form a hairpin have been studied in the constant force ensemble. Using Langevin dynamics simulations, we obtained the force-temperature diagram, which differs from the theoretical prediction based on the lattice model. Probability analysis of the extreme bases of the stem revealed that at high temperature, the hairpin to coil transition is entropy dominated and the loop contributes significantly in its opening. However, at low temperature, the transition is force driven and the hairpin opens from the stem side. It is shown that the elastic energy plays a crucial role at high force. As a result, the force-temperature diagram differs significantly with the theoretical prediction. © *2011 American Institute of Physics*. [doi:10.1063/1.3609970]

I. INTRODUCTION

In recent years, considerable experimental, theoretical, and numerical efforts have been made to understand the dynamics and kinetics of DNA/RNA hairpin.[1–9] This is because the hairpin participates in many biological functions, e.g., replication, transcription, recombination, protein recognition, gene regulation, and in understanding the secondary structure of RNA molecules.[10–13] Moreover, it has been used as a tool in the form of molecular beacon, which provides increased specificity of target recognition in DNA and RNA.[2,3,14–17]

The hairpin is made up of a single stranded DNA (ssDNA)/RNA, which carries sequence of bases that are complementary to each other in each of its two terminal regions. When the base pairing of these two remote sequences are formed, it gives rise to the structure of hairpin, consisting of two segments: a stem, which comprises a short segment of the DNA helix and, a loop of single strand carrying the bases that are not paired (Fig. 1). Structures of the hairpin are not static, as they fluctuate among many different conformations. Broadly speaking, all of these conformations may be classified into the two states: (i) the open state and (ii) the closed state (Fig. 1). The open state has high entropy because of the large number of conformations accessible to the ssDNA, whereas the closed state is a low-entropy state, where enthalpy is involved in the base pairing of the stem. It was shown that the closed-to-open transition requires a sufficiently large amount of energy to unzip all of the base pairs of the stem, whereas the open-to-close transition involves a lower energy barrier.[2,3,18,19] The thermodynamics and kinetics of the hairpin are well studied.[2,3] The melting temperature (T_m) of the hairpin, at which the stem is denatured and the hairpin behaves like a single polymer chain, is measured by fluorescence correlation spectroscopy and in good agreement with theory.[2,3,18] It was also found that the rate of closing strongly depends on the properties of the hairpin loop, such

as length and rigidity, whereas the rate of opening remains relatively insensitive to these properties.[2,3,18]

Single molecule force measuring techniques can manipulate biomolecules (DNA, protein etc.) by applying a force on the pico-newton (pN) scale.[20–24] These techniques such as atomic force microscope, optical tweezers, magnetic tweezers etc. have enhanced our understanding about the structural and functional properties of biomolecules and shed important information about the molecular forces involved in the stability of biomolecules.[20–23] In the case of the DNA hairpin, if the applied force is close to a critical value, then the hairpin fluctuates between the closed and open state. Therefore, efforts were mainly made to understand the kinetics of the hairpin in presence of the applied force.[24–26] These studies suggest that the average dissociation force increases logarithmically with the pulling speed.[26]

To have a better understanding of the biological processes, theoretical works[27–30] focused on simple models, which are either analytically solvable or accurate solution is possible through the extensive numerical simulations. Theoretical analysis of the elasticity of a polymer chain with hairpins as secondary structures[27] reproduces the experimental
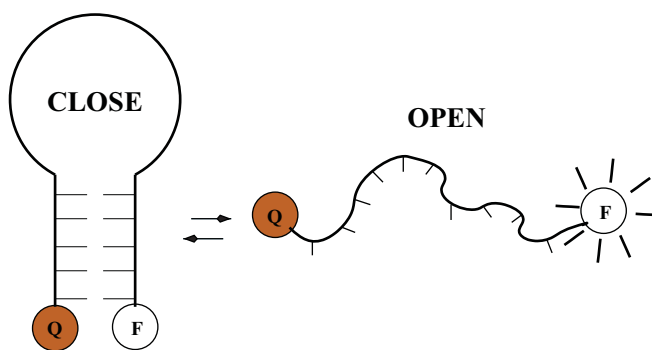

FIG. 1. The schematic representations of the ssDNA which can form a hairpin consisting of stem (complementary nucleotides at two ends) and a loop (made up of non-complementary bases). The hairpin fluctuates between the close and open state.

a)Author to whom correspondence should be addressed. Electronic mail: dgiri99@yahoo.com.
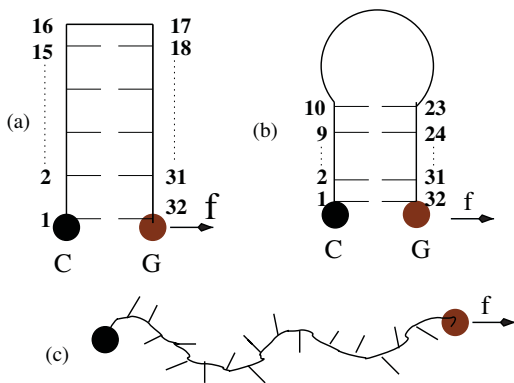
FIG. 2. The schematic representations of transformation of the ssDNA to (a) the dsDNA, (b) a hairpin consisting of a loop and stem, and (c) the extended state. The loop consists of non-complementary nucleotides of the stem.

force-extension curve measured on the ssDNA chains, whose nucleotide bases are arranged in a relatively random order. The force induced transition in the hairpin is found to be of second order and characterized by a gradual decrease in the number of base pairs as the external force increases. Zhou *et al.*[28,29] studied the secondary structure formation of the ssDNA (or RNA) both analytically as well as by the Monte Carlo simulations. They showed that the force induced transition is continuous from the hairpin-I (small base stacking interaction) to the coil, while a first order for the hairpin-II (large base stacking interaction). Hugel *et al.*[30] studied three different chains, namely, ssDNA, poly vinylamine, and peptide at very high force ($\sim$ 2 nN). At such a high force, conformational entropy does not play a significant role, therefore, zero temperature *ab initio* calculation has been applied to compare the experimental results.

In many biological reactions, a slight change in temperature causes a large change in the reaction coordinates.[31] Therefore, efforts of single molecule force spectroscopy experiments have now been shifted to study the effect of temperature keeping the applied force constant. In this respect, Danilowicz *et al.* have measured the critical force required for the unzipping of double stranded DNA (dsDNA) by varying temperature and determined the force-temperature diagram.[32] In another work,[31] it was shown that the elastic properties of ssDNA, which can form a hairpin, have significant temperature dependence. It was found that at the low force, the extension increases with temperature, whereas at the high force, it decreases with temperature. It was argued that the increase in the extension is the result of the disruption of hairpins. However, there is no clear understanding about the decrease in the extension with temperature, at high force. Moreover, the experimental force-temperature diagram of DNA hairpin remains elusive in the literature.

As pointed above, effect of loop length, sequence, nature of transition, and the force-extension curve of DNA/RNA hairpin are well studied at room temperature. In one of the earlier studies,[2] fluorescence and quencher were attached to the two ends of the stem with the assumption that the hairpin opens from the stem-end side.[33] However, if the applied force is constant and temperature varies, the loop entropy may

play a crucial role, whose effect to the best of our knowledge has not been addressed so far. In this paper, we focus mainly on two issues: (i) whether the force-temperature diagram of DNA hairpin differs significantly with the dsDNA or not (Ref. 34–38 yielded qualitatively similar diagram), and (ii) precise effect of loop on the opening of DNA hairpin. In order to study such issues, we introduce a model of polymer with suitable constrain to model the dsDNA and DNA hairpin and performed Langevin dynamics (LD) simulations[39–41] to obtain the thermodynamic observables, which have been discussed in Sec. II. In Sec. III, we validate the model, which describes some of the essential properties of DNA melting. In this section, we also show that the force induced melting of the hairpin differs significantly from the dsDNA. Section IV deals with the semi-microscopic mechanism involved in the opening of the hairpin. Here, we discuss various properties of loop, e.g., entropy, length, and stiffness and its consequence on the opening. We also revisited lattice models in this section and discussed a possible reason for discrepancies in the force-temperature diagram. Finally in Sec. V, we summarize our results and discuss the future perspective.

II. MODEL AND METHOD

The typical time scale involved in the hairpin fluctuations varies from ns to μs, therefore, an all-atom simulation of the longer base sequences is not amenable computationally.[30,42] In view of this, we adopt a minimal off-lattice coarse grained model of the DNA, where a bead represents a few bases associated with sugar and phosphate groups. In order to study the consequences of the loop entropy on the force-temperature diagram, we have considered a ssDNA which can form either a zipped conformation with no bubble/loop (Fig. 2(a)) or a hairpin (Fig. 2(b)) in the chain depending on the base sequence. For the zipped conformation, the first half of the chain (say made up of adenine **C**) interacts with the complimentary other half of the chain (made up of thymine **G**). The ground-state conformations resemble the zipped state of the dsDNA with no loop (Fig. 2(a)). However, if first few beads of the chain are complimentary to the last beads and remaining nucleotides non-complimentary, we have the possibility of the formation of a hairpin (Fig. 2(b)) consisting of a stem and a loop at low temperature. In high force limit, the ssDNA acquires the conformation of the stretched state (Fig. 2(c)). Further refinements in the model requires inclusion of the excluded volume effect and proper base pairing. In addition, the elastic energy and the loop entropy, which play a crucial role in high force and high temperature regimes of the phase diagram, should also be incorporated in the description of the model. The energy of the model system is defined as[43]

$$E = \sum_{i=1}^{N-1} k(d_{i,i+1} - d_0)^2$$

$$+ \sum_{i=1}^{N-2} \sum_{j>i+1}^{N} 4 \left(\frac{B}{d_{i,j}^{12}} - \frac{A_{ij}}{d_{i,j}^{6}} \right) + k_\theta (\theta - \theta_0)^2, \quad (1)$$

TABLE I. Native matrix elements ($A_{i,j}$) of Eq. (1) for two conformational possibilities: a dsDNA and a DNA hairpin.

Case	$A_{1,32}$	$A_{2,31}$	$A_{3,30}$	$A_{4,29}$	$A_{5,28}$	$A_{6,27}$	$A_{7,26}$	$A_{8,25}$	$A_{9,24}$	$A_{10,23}$	$A_{11,22}$	$A_{12,21}$	$A_{13,20}$	$A_{14,19}$	$A_{15,18}$
dsDNA	1	1	1	1	1	1	1	1	1	1	1	1	1	1	1
DNA hairpin	1	1	1	1	1	1	1	1	1	0	0	0	0	0	0

where N is the number of beads. The distance between beads d_{ij}, is defined as $|\vec{r}_i - \vec{r}_j|$, where $\vec{r}_i$ and $\vec{r}_j$ denote the position of bead i and j, respectively. The harmonic term with spring constant k couples the adjacent beads along the chain. We fixed $k = 100$, because the strength of the covalent bond is almost 100 times stronger than the hydrogen bonding.[44] The second term corresponds to the Lennard-Jones (LJ) potential. The first term of LJ potential takes care of the "excluded volume effect," where we set $B = 1$. It should be noted that the hydrogen bonding is directional in nature[45] and only one pairing is possible between two complementary bases. However, the model developed here is for the polymer, where a bead can interact with all the neighboring beads. In order to model DNA, one can assign the base pairing interaction $A_{ij} = 1$ for the native contacts (Table I) and 0 for the non-native ones,[43] which corresponds to the Go model.[46,47] By the "native," we mean that the first base interacts with the Nth (last one) base only and the second base interacts with the $(N-1)$th base and so on as shown in Figs. 2(a) and 2(b). This ensures that the two complimentary bases can form at most one base pair. The remaining term of the Eq. (1) is the bending energy term, which is assigned to successive bonds in the loop only. Here, k_θ is the bending constant and θ is the angle between two consecutive bonds. θ_0 is its equilibrium value. In our subsequent analysis, we will consider two cases, namely, $k_\theta = 0$, which corresponds to a loop made up of thymine and $k_\theta \neq 0$ that corresponds to adenine.[3,48,49] The Go model[46,47] built on the assumption that the "energy" of each conformation is proportional to the number of native contacts, it poses and non-native contacts incur no energetic cost. By construction, the native state is the lowest energy conformation of the zipped state of DNA or DNA hairpin. Since, Go model exhibits a large energy gap between closed to open state and folds rapidly to its ground state, therefore, it saves computational time.

It should be noted here that the model does not include the energetic of the slipped and partially mismatched conformations. A more sophisticated model,[50] which includes directionality of bases and takes care of proper base pairing (non-native interaction), gives rise to the existence of intermediate states in the form of slipped and partially mismatched states. However, for both the models, it was shown that the thermodynamic observables are almost the same for the DNA unzipping.[50] In view of this, we prefer native base pairing interaction in the present model. The parameter $d_0(= 1.12)$ corresponds to the equilibrium distance in the harmonic potential, which is close to the equilibrium position of the average LJ potential. In the Hamiltonian (Eq. (1)), we use dimensionless distances and energy parameters. The major advantage of this model is that the ground-state conformation is known. We obtained the dynamics by using the following

Langevin equation,[39,40,43,51]

$$m\frac{d^2r}{dt^2} = -\zeta\frac{dr}{dt} + F_c + \Gamma, \qquad (2)$$

where m and ζ are the mass of a bead and the friction coefficient, respectively. Here, F_c is defined as $-\frac{dE}{dr}$ and the random force Γ is a white noise,[40] i.e., $\langle\Gamma(t)\Gamma(t')\rangle = 2\zeta T\delta(t-t')$. The choice of this dynamics keeps T constant throughout the simulation for a given f. The equation of motion is integrated using the 6th order predictor corrector algorithm with a time step $\delta t = 0.025$.[40] We add an energy $-\vec{f}.\vec{x}$ to the total energy of the system given by Eq. (1).

We calculate the thermodynamic quantities after the equilibration using the native state as a starting configuration. The equilibration has been checked by calculating the autocorrelation function of any observable q, which is defined as[52,53]

$$\hat{S}_q(t) = \frac{\langle q(0)q(t)\rangle - \langle q(0)\rangle^2}{\langle q^2(0)\rangle - \langle q(0)\rangle^2}. \qquad (3)$$

Here, q can be the end-to-end distance square or the radius of gyration square. The asymptotic behavior of $\hat{S}_q(t)$ for large t is

$$\hat{S}_q(t) \sim \exp\left(-\frac{t}{\tau_{exp}}\right), \qquad (4)$$

where τ_{exp} is so called the (exponential) auto-correlation time. In general, the equilibration can be achieved after $2\tau_{exp}$.[52,53] In our simulation, we have chosen the equilibration time which is ten times more than the τ_{exp}. The data has been sampled over four times of the equilibration time. We have used 2×10^9 time steps out of which the first 5×10^8 steps have not been taken in the averaging. The results are averaged over many trajectories which are almost the same within the standard deviation. We also notice that at low T, it is difficult to achieve the equilibrium, since the applied force probes the local minima instead of global minima.

III. RESULTS

A. Equilibrium property of dsdNA and DNA hairpin at $f = 0$

Before we discuss the underlying physics behind the force-induced transition, we would like first to validate our model based on Eq. (1) and show that the model does include some of the essential features of DNA and melting shows the two state behavior. The reaction coordinate, i.e., absolute value of end-to-end distance ($|x|$) of DNA hairpin and dsDNA have been plotted as a function of temperature in Fig. 3. At low temperature, the thermal energy is too small
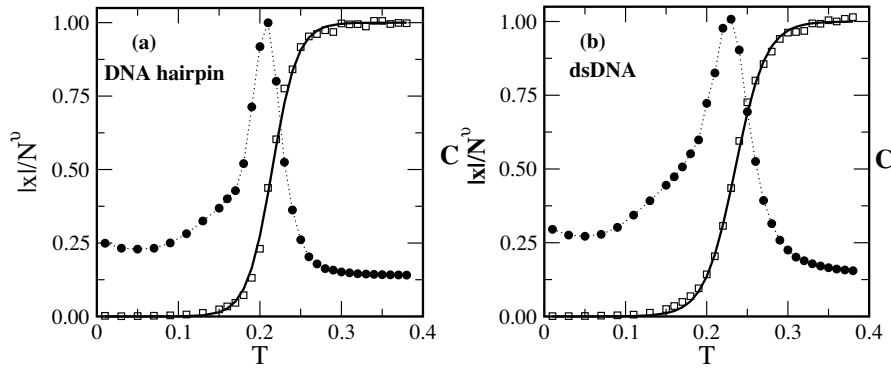
FIG. 3.   Variation of normalized extension(open square) and specific heat (C) (filled circle) with temperature. Solid line corresponds to the sigmoidal fit. (a) for DNA hairpin case (b) for dsDNA case.

to overcome the binding energy and DNA hairpin (dsDNA) remains in the closed state (zipped state), and end-to-end distance remains quite small. At high temperature, the thermal energy is quite large compare to its binding energy and the chain acquires the conformations corresponding to the swollen state (open state), where $|x|$ scales with N^ν. Here ν is the end-to-end distance exponent and its value is given by $3/(d+2)$.[54] The variation $|x|/N^\nu$ can be fitted by the sigmoidal distribution[8] with the melting temperature $T_m = 0.21$ and 0.23 for DNA hairpin and dsDNA, respectively. The melting temperature can also be obtained by monitoring the energy fluctuation (ΔE) or the specific heat (C) with temperature, which are given by the following relations:[43]

$$\langle \Delta E \rangle = \langle E^2 \rangle - \langle E \rangle^2, \qquad (5)$$

$$C = \frac{\langle \Delta E \rangle}{T^2}. \qquad (6)$$

The peak in the specific heat curve gives the melting temperature that matches with the one obtained by the sigmoidal distribution of end-to-end distance. This shows that for a small system transition is well described by the two state model.

B. Force induced melting

In many biological reactions involve a large conformational change in the mechanical reaction coordinate, *i.e.,* $|x|$ or the number of native contacts, that can be used to follow the progress of the reaction.[55] As discussed above, the two state model describes these processes quite effectively in the absence of force. The applied force tilts the free energy surface along the reaction coordinate by an amount linearly dependent on the reaction coordinates.[23,55] One of the notable aspects of the force experiments on a single biomolecule is that $|x|$ is directly measurable or controlled by the instrumentation, therefore, $|x|$ becomes a natural reaction coordinate for describing the mechanical unzipping.

The critical unzipping force, which is a measure of the stability of the DNA hairpin (dsDNA) compared to the open state, has been determined by using Eqs. (5) and (6) as a function of temperature. The state boundary in the force-temperature diagrams (Figs. 4(a) and 4(b)) separate

the regions, where DNA hairpin (dsDNA) exists in a closed state (zipped for dsDNA) from the region where it exists in the open state (unzipped state). It is evident from the plots (Figs. 4(a) and 4(b)) that the melting temperature decreases with the applied force in accordance with the earlier studies.[35–38] The peak position of ΔE and C coincides and the peak height increases with the chain length (26, 32, and 42, where the ratio of stem to loop has been kept constant). However, the transition temperature (melting temperature) remains almost the same in the entire range of f. Since, experiments on hairpin are mostly confined to small chains,[1–3, 24] here, we shall confine ourself to the chain of 32 beads to study the force-temperature diagram and related issues.

For the sake of comparison, in Figs. 4(c) and 4(d), we also show the force-temperature diagram of DNA hairpin (stem length = 3, loop length = 12, and bond length = 2) and dsDNA of 9 base pairs on the cubic lattice using exact enumeration technique.[34] The force-temperature diagrams were found to be in qualitative agreement with earlier theoretical predictions.[35,37,38,49] Despite the simplicity involved in the lattice model, it provides a deeper insight in the mechanism involved in the force induced transitions.[23] A self attracting self-avoiding walk on appropriate lattice (here cubic lattice) may be used to model a DNA hairpin (stem and loop) and dsDNA (zipped). The base pairing is assigned ($\epsilon = -1$), when the two complimentary nucleotides are on the nearest neighbor. The nearest neighbor interaction mimics the short range nature of the hydrogen bonds, which are qualitatively similar to the model adopted here.

It is pertinent to mention here that for the small base pair sequences (< 100), the differential melting curve of the dsDNA shows a single peak,[56] indicating a sudden unbinding of two strands. Since for the short dsDNA, the entropy contributions of spontaneous bubbles are not very important as loops are rare, therefore, transition is well described by the two state model.[56] One would expect that the force-temperature diagram of the short dsDNA presented here should then match with the two state model. The free energy of the unzipped chain (g_u) under the applied force can be obtained through the freely jointed chain (FJC) model,[57]

$$g_u^{FJC} = \frac{l}{b} k_b T \ln\left[\frac{k_b T}{fb}\sinh\left(\frac{fb}{k_b T}\right)\right], \qquad (7)$$
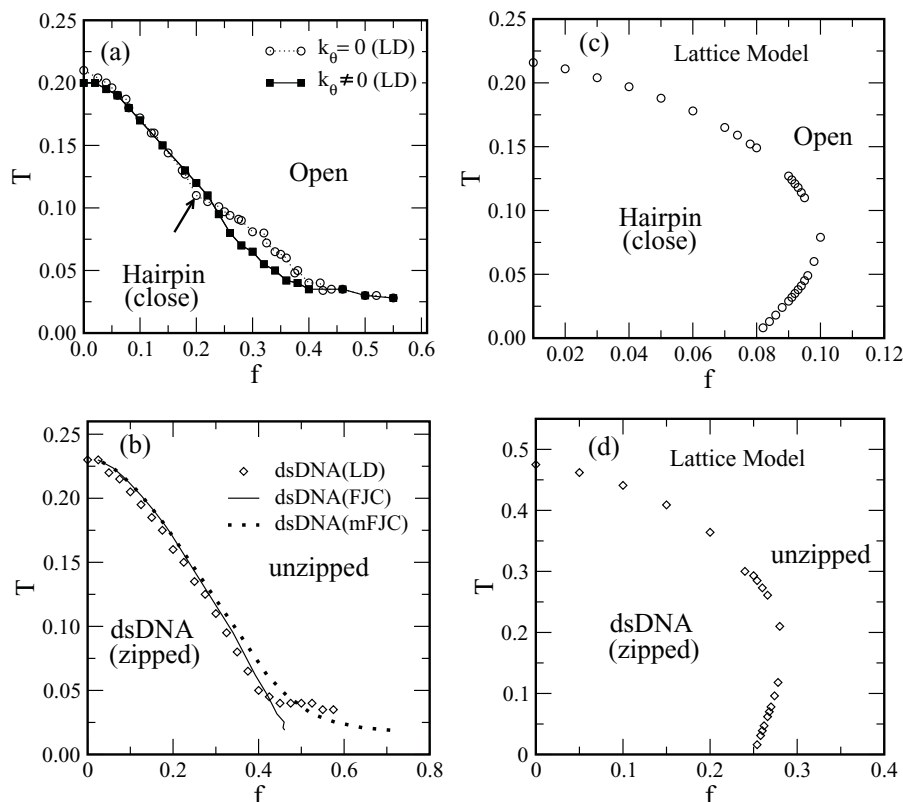
FIG. 4. (a) $f - T$ diagrams for a DNA hairpin obtained from LD simulations with and without the bending energy term. The arrow indicates the change in the slope which vanishes for $k_\theta = 20$; (b) $f - T$ diagrams for the dsDNA using LD simulations. The force-temperature diagram is also compared with the FJC and the mFJC models in the reduced unit. Our results are in good agreement with the FJC and the mFJC. The deviation at high force is because of the elastic energy, which is included in the mFJC; (c) and (d) The force-temperature diagrams for the DNA hairpin and the dsDNA using lattice model, which are qualitatively similar to each other. Clear differences between simulation and lattice model are visible at intermediate and high force regime of the force-temperature diagram.

which can be compared with the bound state energy (g_b) of the dsDNA to get the force-temperature diagram, which is shown in Fig. 4(b). Here, b and l are the Kuhn length and bond length of the chain, respectively. In the reduced unit for the dsDNA, one can notice a nice agreement between the off-lattice simulation presented here and the two state model (Eq. (7)) over a wide range of f and T. However, at low T and high f, the state boundary deviates from the FJC model. One should recall that the first term of the Hamiltonian defined in Eq. (1) may induce the possibility of the stretched state at high force, where the bond length may exceed than its equilibrium value. In fact in the FJC model, the bond length is taken as a constant. It should be emphasized here that the modified freely jointed chain (mFJC) model does include the possibility of the stretching of bonds in its description.[32,58] Therefore, if this deviation is because of the elastic energy then the two state model based on the mFJC model should show a similar behavior as seen in the simulation. The free energy of the unbound state of the mFJC may be obtained by including $(l/2b)((f\ell)^2/k_b T)$ term in Eq. (5),[32,58] where ℓ is the increase in the bond length. The corresponding force-temperature diagram in the reduced unit shown in Fig. 4(b) is in excellent agreement with the simulation in the entire range of f and T.

The off-lattice simulation performed here, clearly shows the effect of loop of the hairpin on the melting profile. The force-temperature diagram of the hairpin (Fig. 4(a)) differs

significantly from the dsDNA (Fig. 4(b)) as well as deviates considerably with the counter lattice model of the hairpin (Fig. 4(c)). Two major differences can be noticed from the figures: (i) a change in the slope at the intermediate value of force for the hairpin (Fig. 4(a)), which is absent (Fig. 4(b)) in the case of dsDNA (no loop) as well as in the previous theoretical models;[35–38] (ii) an abrupt increase in the force for both the hairpin and the dsDNA at low temperature (Figs. 4(a) and 4(b)), whereas the lattice model and other theoretical studies[35–38] show the re-entrance for both hairpin and dsDNA (Figs. 4(c) and 4(d)).

To have further understanding of it, we have monitored the reaction coordinate ($|x|$) of the hairpin with temperature at different values of f (Fig. 5). At low f, transition is weak due to the finite width of the melting profile, which decreases with f. At high f, however, it shows a strong first order characteristic. At high force, the non-monotonic behavior of the extension with temperature as observed in a recent experiment[31] is also evident from Fig. 5. As T increases, the chain acquires the stretched state (Fig. 2(c)) because of the applied force. A further rise in T results an increase in the contribution of the configurational entropy of the chain. The applied force is not enough to hold the stretched conformation and thus the extension falls.[34,59] At intermediate f (~ 0.19) where the change in the slope is observed (Fig. 4(a)), we find that the entropic ($T\,dS$) and the
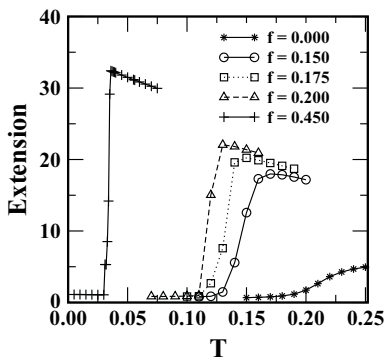
FIG. 5. Temperature-extension curves at different values of the force.

FIG. 7. Variation of the applied force with loop length at high and low temperatures.

force ($f \, dx$) contributions to the free energy are nearly the same.

At constant temperature, by varying f, the system attains the extended states from the closed state of the hairpin. With further rise of f, one finds the stretched state, i.e., the extension approaches the contour length of the ssDNA. At high T, when f increases hairpin goes to the extended state. At the same T, if we decrease the applied force, the system retraces the path to the closed state without any hysteresis. Because of high entropy, it is possible that monomers of two segments of strand come close to each other and re-zipping takes place (Fig. 7(a)). As we decrease the T below 0.15, by increasing f, hairpin acquires the stretched state. Interestingly, now it does not retrace the path if f decreases at that T (Fig. 7(b)). This is the clear signature of hysteresis. It is because of the contribution of entropy, which is not sufficient enough to bring two ends close to each other so that re-zipping can take place. The hysteresis has been measured recently in unzipping and re-zipping of DNA.[60] It was found that the area of hysteresis loop increases with decreasing temperature, which is also consistent with our findings (Fig. 6(b)).

IV. EFFECT OF LOOP ON THE OPENING OF HAIRPIN

The thermodynamics of DNA melting is well studied using the following equation:[61]

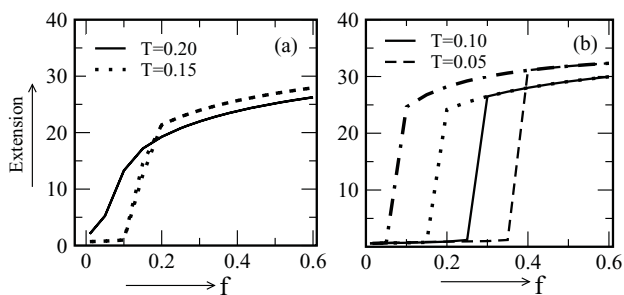$$\Delta G = \Delta H - T \, \Delta S_{stem} - T \, \Delta S_{loop}, \qquad (8)$$

FIG. 6. Variation of extension (up to contour length) with f at $T > 0.15$. The path retraces and there is no signature of hysteresis; (b) same as (a), but at $T < 0.15$. Path does not retrace with decreasing f and a force is required to re-zip, which is a signature of hysteresis (dotted and dotted-dashed line) .
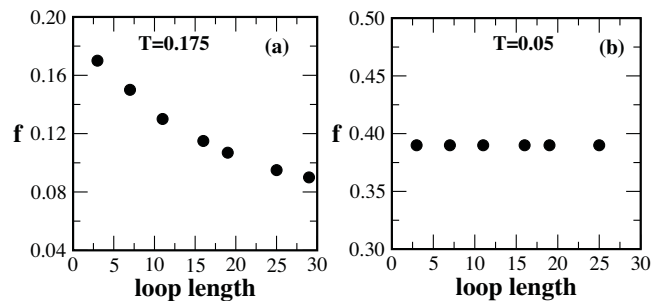
where G, H, S_{stem}, and S_{loop} are the free energy, enthalpy, entropy associated with stem and loop, respectively. To determine the entropic force of the loop, we fix the stem length and vary the loop length from 0 to N/2 at fixed T. Since the contribution of first two term of Eq. (8) remains constant as stem length is kept fixed, the decrease in the applied force is the result of the loop entropy. In Fig. 7, we plot the force as a function of loop length at two different temperatures. At high temperature, the loop entropy reduces the applied force (Fig. 7(a)), and hence, there is decreases in the force, which is in accordance with recent experiment.[24] However, at low temperature, the applied force remains constant (Fig. 7(b)) indicating that the loop entropy does not play any role in the opening of the hairpin and opening is mainly force driven. This is because at low temperature, applied force probes the local minima and hence remain independent of global minima. However, re-zipping force does depend on the loop length.

In order to substantiate our findings, we tracked the first ($1 - 32$, stem-end) and the last ($10 - 23$, loop-end) base pairs of the stem (Fig. 2(b)) in different regimes of the $f - T$ diagram. In Fig. 8, we show the probability of opening (P_o) of the stem-end and the loop-end base pairs with f at a given T. Near the state boundary, at high T, transition from the hairpin to the coil state is entropy driven as discussed above. This is apparent from Fig. 8(a), where P_o for the loop-end is higher than that of the stem-end. This indicates that in the opening of the hairpin, the loop contributes significantly compared to the applied force. At intermediate T (~ 0.12), P_o of the stem-end and the loop-end are comparable, reflecting that the hairpin can open from any sides (Fig. 8(b)). However, at low T, the dominant contribution in the opening of hairpin comes from the stem-end side and the transition is force driven (Fig. 8(c)).

It remains a matter of quest that why the exact solution of the lattice models of hairpin[34] could not exhibit this feature. This prompted us to revisit the lattice model studied in Ref. 34. We calculated P_o of the stem-end and the loop-end for the lattice model of the hairpin. At high T, opening of the hairpin, the dominant contribution comes from the stem side of the hairpin. This should not be taken as surprise as lattice models do not take the loop entropy properly in their description. In fact, the discrete nature of the lattice (coordination number) reduces the loop entropy. The model studied here is the off-lattice one, where the loop entropy has been taken properly into account assuming that ssDNA is well described by the FJC model.[21,58] Therefore, this behavior occurs in our model system.
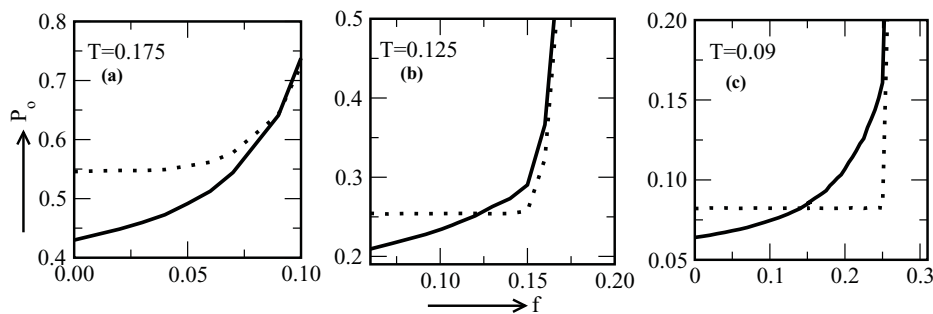
FIG. 8. (a) Comparison of the probability of opening (P_o) of the stem-end (solid line) and the loop-end (dotted line) with the force for different temperatures. Near the transition point (Fig. 4(a)), the probability of opening is higher for the loop-end; (b) The two probabilities are comparable, and hence, the hairpin can open from both sides; (c) It reflects that opening is always from the stem-end side.

If the change in the slope (Fig. 4(a)) is because of the loop entropy (underestimated in the lattice models), then the change in the slope should also vanish even in the off-lattice model, if the loop entropy is reduced somehow. This can be achieved by putting $k_\theta \neq 0$ in the loop (Eq. (1)). We repeated the simulation with the bending constant k_θ in between 10 and 20, which has been used in earlier simulations.[44,62,63] Because of this term, the change in the slope seen at intermediate value of f vanishes (Fig. 4(a)). The most striking observation here is that the probability distribution analysis shows that the opening of hairpin is contributed by the stem-end side, even at high temperature.

V. CONCLUSIONS

In conclusion, we have studied a simple model of a polymer, which can form a dsDNA or a DNA hairpin depending on the interaction matrix given in Table I. The model includes the possibility of the stretched state in its description. Since, simulation is performed on the off-lattice, therefore, the loop entropy has been taken properly into account in case of the hairpin. The $f - T$ diagrams of the hairpin differs significantly from the dsDNA as well as previous studies.[34–38]

We show that the loop entropy plays an important role, which has been underestimated in previous studies. This conclusion is based on the probability analysis of the extreme bases of the stem (loop-end and stem-end), which rendered the semi-microscopic mechanism involved in the force induced melting. Our results provide support for the existence of the apparent change in the slope in the force-temperature diagram. In the intermediate range of f and T, a chain can open from both sides, reflecting that the entropic and force contributions are nearly the same, which may be verified experimentally. At high T, the transition is entropy dominated and the loop contributes in the opening of hairpin (Fig. 6(a)). At low T, it is force driven and it opens from the stem-end side (Fig. 6(b)). It should be noted here that, in the description of the lattice model, the critical force for DNA hairpin near $T = 0$ differs significantly with dsDNA (Figs. 4(c) and 4(d)), where as in the simulation the unzipping forces for both the cases were found nearly the same (Figs. 4(a) and 4(b)). This should not be taken as a surprise because in the exact enumeration, one has the complete information of the partition function and hence the global minimum can be obtained to

calculate the critical force at low T. However, in present simulation, we follow the experiments and report the dynamical force required to unzip the chain in Figs. 4(a) and 4(b) and Fig. 7,[60,64] which probes the local minima at low T. This force may differs with the critical force at low T. For example, for the 50 000 bases $\lambda-$DNA, the critical force was found to be 15.5 pN to overcome the energy barrier $\sim 3000\ K_B T$. Full opening of the molecule never happens in the experiment as time required to open the barrier is quite large. Thus, a larger force (17 pN) than its critical force is required to open a finite fraction[65] of the chain.

It is important to mention here that a change in the phase boundary has also been observed in the force induced unzipping of λ-phage dsDNA consisting of ∼1500 base pairs. For such a long chain, differential melting curve shows several peaks corresponding to the partial melting of dsDNA, which form spontaneous bubbles in the chain.[56] This suggests that for a longer chain, formation of spontaneous bubble should be incorporated in the model. Using Peyrard-Bishop-Dauxois (PBD) model,[66] Voulgarakis et al.[67] probed the mechanical unzipping of dsDNA with bubble. One of the important results they derived, is that the single strand as it extends between the dsDNA causes a decrease in the measured force but the $f - T$ diagram remains significantly different than the experiment. Recalling that in the PBD model, a bead can move only in one-dimension, and hence the entropy of the loop is also underestimated here, which may be the reason for such difference. Therefore, at this stage of time a simulation of longer base sequences is required, which should have spontaneous bubbles in its description with proper entropy to settle this issue.

The another interesting finding of our studies is the absence of re-entrance at low temperature. The basic assumption behind the theoretical models or phenomenological argument is that the bond length in the model system is a constant. However, recent experiments[32,48] suggests that there is a net increase in the bond length at high force. Consequently, model studied here incorporates the simplest form of the elastic energy (i.e., Gaussian spring). We have kept the spring constant quite large in our simulation to model the covalent bond. The experimental force-temperature diagram of $\lambda-$phage DNA (Ref. 32) shows the similar behavior at high force. The observed decrease in the slope at low temperature in the experiment is attributed to a thermally induced change

in the dsDNA conformation.[32] However, present simulation (DNA hairpin and dsDNA) along with the two state model based on the mFJC suggests that such deviation may be because of the elastic energy. In earlier studies, either this energy has not been included in the models[66–68] or the bond length has been taken as a constant,[34–37] thus precluding the existence of the stretched state with the increased bond length in both cases (dsDNA and hairpin). Consequently, these models could not describe this feature of abrupt increase in the force at low T. In future theoretical studies, one may use finite extensible nonlinear elastic potential[69] and proper loop entropy, e.g., one used in Ref. 70 to have further understanding of the force-temperature diagram of a longer dsDNA.

ACKNOWLEDGMENTS

[1] M. I. Wallace, L. Ying, S. Balasubramanian, and D. Klenerman, Proc. Natl. Acad. Sci. U.S.A. **98**, 5584 (2001).

[2] G. Bonnet, O. Krichevsky, and A. Libchaber, Proc. Natl. Acad. Sci. U.S.A. **95**, 8602 (1998).

[3] N. L. Goddard, G. Bonnet, O. Krichevsky, and A. Libchaber, Phys. Rev. Lett. **85**, 2400 (2000).

[4] W. B. Zhang and S. J. Chen, Proc. Natl. Acad. Sci. U.S.A. **99**, 1931 (2002).

[5] J. Kim, S. Doose, H. Neuweiler, and M. Sauer, Nucleic Acids Res. **34**, 2516 (2006).

[6] L. G. Nivon and E. I. Shakhnovich, J. Mol. Biol. **344**, 29 (2004).

[7] M. M. Lin, L. Meinhold, D. Shorokhov, and A. H. Zewail, Phys. Chem. Chem. Phys. **10**, 4227 (2008).

[8] M. Kenward and K. D. Dorfman, J. Chem. Phys. **130**, 095101 (2009).

[9] J. Errami, M. Peyrard, and N. Theodorakopoulos, Eur. Phys. J. A **23**, 397 (2007).

[10] E. Zazopoulos, E. Lalli, D. M. Stocco, and P. Sassone-Corsi, Nature (London) **390**, 311 (1997).

[11] S. J. Froelich-Ammon, K. C. Gale, and N. Osheroff, J. Biol. Chem. **269**, 7719 (1994).

[12] T. Q. Trinh and R. R. Sinden, Genetics **134**, 409 (1993).

[13] J. Tang, J. Temsamani, and S. Agrawal, Nucleic Acids Res. **21**, 2729 (1993).

[14] W. H. Tan, K. M. Wang, and T. J. Drake, Curr. Opin. Chem. Biol. **8**, 547 (2004).

[15] N. E. Broude, Trends Biotechnol. **20**, 249 (2002).

[16] Y. S. Li, X. Y. Zhou, and D. Y. Ye, Biochem. Biophys. Res. Comm. **373**, 457 (2008).

[17] T. J. Drake and W. H. Tan, Appl. Spectroscopy **58**, 269A (2004).

[18] Y.-J. Sheng, J. Z. Y. Chen, and H.-K. Tsao, Macromolecules **35**, 9624 (2002); Y.-J. Sheng, P.-H. Hsu, J. Z. Y. Chen, and H.-K. Tsao, Macromolecules **37**, 9257 (2004).

[19] A. Sain, B.-Y. Ha, H.-K. Tsao, and J. Z. Y. Chen, Phys. Rev. E **69**, 061913 (2004); Y. J. Sheng, H. J. Lin, J. Z. Y. Chen, and H. K. Tsao, J. Chem. Phys. **118**, 8513 (2003).

[20] U. Bockelmann, B. Essevaz-Roulet, and F. Heslot, Phys. Rev. Lett. **79**, 4489 (1997).

[21] S. B. Smith, Y. Cui, and C. Bustamante, Science **271**, 795 (1996).

[22] U. Bockelmann, Curr. Opin. Struct. Biol. **14**, 368 (2004).

[23] S. Kumar and M. S. Li, Phys. Rep. **486**, 1 (2010).

[24] M. T. Woodside, W. M. Behnke-Parks, K. Larizadeh, K. Travers, D. Herschlag, and S. M. Block, Proc. Natl. Acad. Sci. U.S.A. **103**, 6190 (2006).

[25] J. Hanne, G. Zocchi, N. K. Voulgarakis, A. R. Bishop, and K. Ø. Rasmussen, Phys. Rev. E. **76**, 011909 (2007).

[26] A. Mossa, M. Manosas, N. Forns, J. M. Huguet, and F. Ritort, J. Stat. Mech.: Theory Expt. **2009**, P02060.

[27] A. Montanari and M. Mezard, Phys. Rev. Lett. **86**, 2178 (2001).

[28] H. Zhou, Y. Zhang, and Z.-C. Ou-Yang, Phys. Rev. Lett. **86**, 356 (2001).

[29] Y. Zhang, H. Zhou, and Z.-C. Ou-Yang, Biophys. J. **81**, 1133 (2001).

[30] T. Hugel, M. Rief, M. Seitz, H. E. Gaub, and R. R. Netz, Phys. ReV. Lett. **94**, 48301 (2005).

[31] C. Danilowicz, C. H. Lee, V. W. Coljee, and M. Prentiss, Phys. Rev. E **75**, 030902(R) (2007).

[32] C. Danilowicz, Y. Kafri, R. S. Conroy, V. W. Coljee, J. Weeks, and M. Prentiss, Phys. Rev. Lett. **93**, 078101 (2004).

[33] J. Ignacio Tinoco, Annu. Rev. Biophys. Biomol. Struct. **33**, 363 (2004).

[34] S. Kumar and G. Mishra, Phys. Rev. E **78**, 011907 (2008).

[35] S. M. Bhattacharjee, J. Phys. A **33**, L423 (2000).

[36] N. Singh and Y. Singh, Eur. Phys. J. E **17**, 7 (2005); Phys. Rev. E **64**, 042901 (2001).

[37] D. Marenduzzo, S. M. Bhattacharjee, A. Maritan, E. Orlandini, and F. Seno, Phys. Rev. Lett. **88**, 028102 (2001).

[38] R. Kapri, S. M. Bhattacharjee, and F. Seno, Phys. Rev. Lett. **93**, 248102 (2004).

[39] M. P. Allen and D. J. Tildesley, *Computer Simulations of Liquids* (Oxford Science, Oxford, UK, 1987).

[40] D. Frenkel and B. Smit, *Understanding Molecular Simulation* (Academic, London, UK, 2002).

[41] J. Schluttig, M. Bachmann, and W. Janke, J. Comput. Chem. **29**, 2603 (2008).

[42] M. Santosh and P. K Maiti, J. Phys.: Condens. Matter **21**, 034113 (2009).

[43] M. S. Li and M. Cieplak, Phys. Rev E **59**, 970 (1999); S. Kumar and Y. Singh, J. Phys. A: Math. Gen. **26**, L987 (1993).

[44] A. Morriss-Andrews, J. Rottler, and S. S. Plotkin, J. Chem. Phys. **132**, 035105 (2010).

[45] I. Rouzina and V. A. Bloomfield, Biophys. J. **80**, 894 (2001); **80**, 894 (2001).

[46] N. Go and H. Abe, Biopolymers **20**, 991 (1981).

[47] E. J. Sambriski, V. Ortiz, and J. J. de Pablo, J. Phys.: Condens. Matter **21**, 034105 (2009).

[48] C. Ke, M. Humeniuk, H. S-Gracz, and P. E. Marszalek, Phys. Rev. Lett. **99**, 018302 (2007).

[49] S. Kumar, D. Giri, and S. M Bhattacahrjee, Phys. Rev. E **71**, 51804 (2005).

[50] D. Giri and S. Kumar, Phys. Rev. E **73**, 050903(R), 2006.

[51] M. S. Li, Biophys. J. **93**, 2644 (2007); M. Kouza, C.-F. Chang, S. Hayryan, T.-H. Yu, M. S. Li, T.-H. Huang, and C.-K. Hu, Biophys. J. **89**, 3353 (2005).

[52] G. E. P. Box and G. M. Jenkins, *Time Series Analysis: Forecasting and Control* (Holden-Day, San Francisco, 1970); Y. S. Lee and T. Ree, Bull. Korean Chem. Soc. **3**, 44 (1982).

[53] B. A. Berg, in *Markov Chain Monte Carlo: Innovations and Applications*, edited by W. S. Kendall, F. Liang, and J.-S. Wang (World Scientific, Singapore, 2005), pp. 1–52.

[54] P. G. de Gennes, *Scaling Concepts in Polymer Physics* (Cornell University, Ithaca, NY, 1979).

[55] C. Bustamante, Y. R. Chemla, N. R. Forde, and D. Izhaky, Annu. Rev. Biochem. **73**, 705 (2004).

[56] R. Wartell and A. Benight, Phys. Rep. **126**, 67 (1985).

[57] T. R. Strick, M.-N. Dessinges, G. Charvin, N. H. Dekker, J.-F. Allemand, D. Bensimon, and V. Croquette, Rep. Prog. Phys. **66**, 1 (2003).

[58] M.-N. Dessinges, B. Maier, Y. Zhang, M. Peliti, D. Bensimon, and V. Croquette, Phys. Rev. Lett. **89**, 248102 (2002).

[59] S. Kumar, I. Jensen, J. L. Jacobsen, and A. J. Guttmann, Phys. Rev. Lett. **98**, 128101 (2007).

[60] K. Hatch, C. Danilowicz, V. Coljee, and M. Prentiss, Phys. Rev E **75**, 051908 (2007).

[61] S. V. Kuznetsov, C.-C. Ren, S. A. Woodson, and A. Ansari, Nucleic Acids Res. **36**, 1098 (2007).

[62] M. Kouza, C.-K. Hu, and M. S. Li, J. Chem. Phys. **128**, 045103 (2008).

[63] A. Noy, A. Perez, F. Lankas, F. J. Luque, and M. Orozco, J. Mol. Biol. **343**, 627 (2004).

[64] C. Danilowicz, V. W. Coljee, C. Bouzigues, D. K. Lubensky, D. R. Nelson, and M. Prentiss, Proc. Natl. Acad. Sci. U.S.A. **100**, 1694 (2003).

[65] S. Cocco, J. F. Marko, and R. Monasson, Eur. Phys. J. E **10**, 153 (2003).

[66] T. Dauxois, M. Peyrard, and A. R. Bishop, Phys. Rev. E **47**, 684 (1993).

[67] N. K. Voulgarakis, A. Redondo, A. R. Bishop, and K. A. Rosmussen, Phys. Rev. Lett. **96**, 248101 (2006).

[68] Y. Kafri, D. Mukamel, and L. Peliti, Europhys. J. B **27**, 135 (2002).

[69] A. Peterlin, Polymer **2**, 257 (1961).

[70] R. Bundschuh and U. Gerland, Phys. Rev. Lett. **95**, 208104 (2005).